Available online at www.sciencedirect.com
SCIENCE DIRECT®
Chemical Physics Letters 375 (2003) 435–443
CHEMICAL PHYSICS LETTERS
www.elsevier.com/locate/cplett

Mapping out the conduction band under CTTS transitions: the photodetachment quantum yield of sodide (Na^-) in tetrahydrofuran

Erik R. Barthel, Benjamin J. Schwartz *

Department of Chemistry and Biochemistry, University of California, Los Angeles, CA 90095-1569, USA

Received 2 May 2003; in final form 28 May 2003

Abstract

Upon photoexcitation of the charge-transfer-to-solvent absorption band of Na^- in tetrahydrofuran (THF), electrons detach into immediate contact pairs, solvent-separated contact pairs, or as free electrons. In this Letter, we analyze the recombination dynamics of Na^- at multiple excitation wavelengths to determine the action spectrum for production of each type of electron. The action spectra match well with the four Gaussian sub-bands (corresponding to three p-like CTTS states and the continuum) needed to describe the polarized bleach recovery. We also find that the Na^- free-electron action spectrum is linearly related to the Rb^-/THF photocurrent action spectrum measured by Levanon and co-workers.

1. Introduction

Photodetachment is a fundamental physical process in which an electron is removed from an atomic or molecular species via irradiation with photons of visible or UV light [1]. In the gas phase, photodetachment spectroscopy can be used to map out the potential energy surfaces of transition states of reactive molecules [2]. In clusters [2,3] and in the liquid phase [4], however, the ground and excited electronic states of a solvated species are strongly coupled to the solvent, resulting in shifting and broadening of absorption lines and allowing for channels of electron detachment other than direct photoejection [5]. In many cases, states which are in the continuum above the detachment threshold in the gas phase can be shifted down to below the vacuum level in clusters or in solution, resulting in strongly allowed optical charge transfer absorption bands. When excitation of such a charge transfer band results in the detachment of an electron from the solute but leaves the electron localized in the surrounding solvent, the absorption band is referred to as a charge-transfer-to-solvent (CTTS) transition [6].

In a recent study, Levanon and co-workers [7] measured the cross-section and quantum yield for electron photodetachment from rubidide (Rb^-) in

* Corresponding author. Fax: 1-310-206-4038.
E-mail address: schwartz@chem.ucla.edu (B.J. Schwartz).

0009-2614/03/$ - see front matter © 2003 Elsevier Science B.V. All rights reserved.
doi:10.1016/S0009-2614(03)00922-9

tetrahydrofuran (THF), which has its CTTS absorption maximum near 1.3 eV. These workers found that the photodetachment cross-section closely follows the molar extinction coefficient. Moreover, Levanon and co-workers also found that the photodetachment quantum yield (the photodetachment cross-section divided by the absorption cross-section) has two separate regimes as a function of excitation energy. At low excitation energies, the number of electrons liberated per photon has a constant value near 0.03, while at higher excitation energies (above ~2.4 eV), the detachment quantum yield reaches a roughly constant plateau at ~0.085. The data were interpreted in terms of a model in which solvent-mediated CTTS is the dominant detachment route for excitation energies below ~1.8 eV, and autoionization of the electron into Anderson-localized states that lie energetically between the THF conduction band and the solvated electron's ground state is the dominant channel for excitation energies above ~2.4 eV [7].

We have performed a series of studies on the photodetachment dynamics of another alkali metal anion in THF, sodide (Na^-) [8–10], whose CTTS band is shown in Fig. 1a. We found that upon photoexcitation, solvent reorganization around the solvent-stabilized CTTS state leads to detachment on a ~1-ps time scale, with the detached electron localized in a nearby solvent cavity [8]. Excitation on the low-energy side of the CTTS band ($\lambda > 730$ nm) primarily creates solvated electrons that reside in the same solvent cavity as their geminate sodium atom partners, which we refer to as 'immediate' contact pairs [10]. Since the wave function of an immediate contact pair electron has significant overlap with the sodium atom in its first solvent shell, immediate contact pairs undergo rapid back electron transfer (recombination) on a ~1-ps time scale [8,10]. Excitation on the high-energy side of the CTTS band, in contrast, can produce solvated electrons that are located one solvent shell away from their parents [9]. Since there is no direct wave function overlap between these 'solvent-separated' contact pair electrons and the nearby sodium atoms, back electron transfer is inhibited and takes place on a hundreds-of-ps time scale [9]. High excitation energies also produce

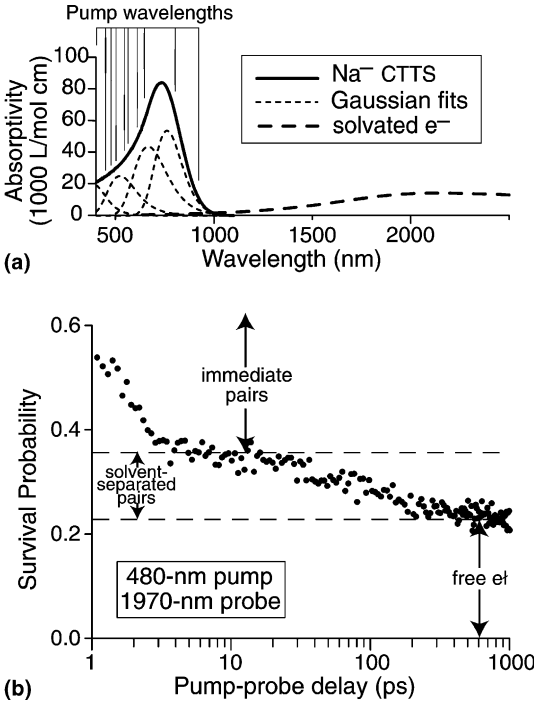

Fig. 1. (a) Absorption spectra of the important species examined in this Letter: the CTTS band of Na^- in THF (solid curve) and the solvated electron in THF (dashed curve). The dotted curves show the four Gaussian sub-bands constituting the Na^- CTTS band; see text for details. The thin vertical lines indicate the 10 excitation wavelengths used in the pump–probe scans. (b) Representative pump–probe scan monitoring the absorbance of the solvated electron in THF at 1970 nm following CTTS excitation of sodide at 480 nm; the data are plotted on a logarithmic time axis (same as Fig. 2h on a linear axis). The labels illustrate the different recombination fractions in the data.

'free' solvated electrons that are ejected to distances farther away than the second solvent shell; free solvated electrons do not recombine on sub-ns time scales [9]. The distinct back electron transfer dynamics of the three different types of CTTS-ejected electrons can be seen in Fig. 1b, which shows the population of THF-solvated electrons monitored via their ~2 μm absorption (cf. Fig. 1a) as a function of time after 480-nm photoexcitation of the Na^- CTTS band. We have verified the existence of three distinct environments for the detached electron by showing that the electrons in each environment respond differently when re-excited in multi-pulse femtosecond experiments [11,12].

In addition to our work, Ruhman and co-workers [13] have found a polarization dependence in the recovery of the bleach of the Na^- CTTS band, suggesting that this band is inhomogeneously broadened. Our group has made similar observations, and we were successfully able to model the polarization dependence by assuming that the CTTS band consists of transitions to three Gaussian quasi-bound CTTS excited states plus a tail due to absorption into the continuum [14], as shown by the short-dashed curves in Fig. 1a. This decomposition of the band makes physical sense: the ground state electron on the Na^- is in a 3s orbital, so the three solvent-bound CTTS excited states should be p-like in nature. If the solvent cavity were perfectly symmetric, these p-like states would be degenerate, but since the cavity is on average more ellipsoidal than spherical, the p-like states are split by the local broken symmetry. This effect also has been observed in solid sodides, where the crystal lattice provides a permanent asymmetry that splits the localized p-like excited states [15]. Thus, we have strong reason to believe that there is a more complex electronic structure underlying the smooth CTTS absorption band of Na^- [13,14].

In this Letter, we will argue that the free electrons produced via photoexcitation of sodide come from the selective excitation of specific sub-bands under the Na^- absorption spectrum. We also present evidence that solvent-separated contact pairs are produced much less frequently than either immediate contact pairs or free electrons, suggesting that localization into a stable solvent-separated state is a relatively rare event. We then show that the way in which the number of free electrons produced following CTTS excitation of sodide varies with excitation energy correlates well with the photodetachment spectrum for Rb^- measured by Levanon and co-workers. All the detachment data fit well with a picture in which there are three different quasi-bound states and a continuum underlying the CTTS absorption band of the alkali metal anions.

The preparation of Na^-/THF solutions has been described in detail elsewhere [8], and is based upon the technique of Dye [16]. The ultrafast pump–probe laser setup used in our lab has also been described in detail previously [17]. In brief, a regeneratively amplified 1-kHz Ti:sapphire laser emitting ~1-mJ pulses of ~100-fs duration at 780 nm (Spectra physics) was used to pump a double-pass optical parametric amplifier that produced tunable signal and idler beams in the infrared. Visible excitation beams throughout the sodide absorption band were produced via sum-frequency mixing of the residual 780-nm light with either the signal or idler beams from the OPA. After reflecting off a computer-controlled variable delay stage, the probe pulses were split into sample and reference beams, which were detected with matched Si (visible light), InGaAs (near IR) or InAs (IR) photodiodes. The output of the photodiodes was digitally locked to the excitation pulse, and normalized on a shot-to-shot basis by a fast-gated current-integrating analog-to-digital converter.

Fig. 2 shows femtosecond pump–probe scans monitoring the dynamics of electron detachment from Na^- in THF following excitation at each of 10 distinct wavelengths throughout the CTTS absorption band (indicated in Fig. 1a). The left panels show the data on a ~10-ps time scale, while the right panels show the same data on a hundreds-of-ps timescale. The data monitor the ejection and recombination kinetics by probing the transient absorption dynamics of the electron, [1] providing a direct measurement of the population of detached electrons [8–10]. The sub-ps rise in the ~2-μm absorbance is attributable to the delayed detachment of the CTTS-excited electron from Na^- [8,9]. The absorption of the electrons then decays on a ~1-ps time scale due to geminate recombination of electrons in immediate contact pairs. On the longer timescale, the data show a ~200-ps (and highly non-exponential) decay due to the recombination of electrons in solvent-separated contact pairs, followed by an offset due to

[1] Note that the 910-nm excitation data in Fig. 2a probe the recovery of the bleach of the CTTS band at 490 nm rather than the 2-μm absorption of the electron. Other than the fact that the appearance of the bleach is instrument-limited, the kinetics of the bleach recovery and the decay of the electron's absorption are identical, as we have shown in [9,10,14].

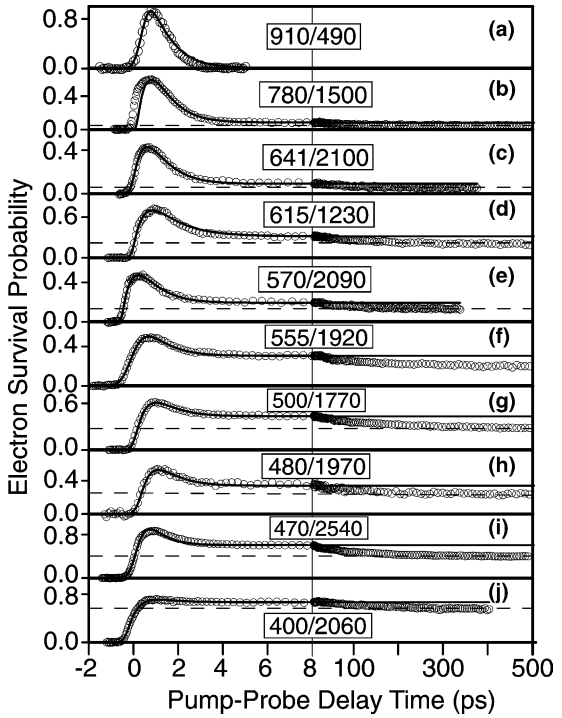

Fig. 2. Short time (left panels) and long time (right panels) recombination dynamics of solvated electrons produced via CTTS of Na^- in THF (circles), with pump and probe wavelengths indicated in the left panel legend for each scan. The solid curves are fits of the short time data to the DE + S model; the dashed lines denote the average of the signal at times longer than 300 ps, corresponding to the fraction of free electrons remaining after immediate and solvent-separated contact pairs have recombined. The difference between the DE + S fit offsets and the dashed lines defines the fraction of electrons detached into solvent-separated contact pairs; see text for details. The long-time data are omitted for the 910-nm scan in panel (a) because there was no signal after 5 ps; the data in this scan used a 490-nm probe wavelength. [2]

persistent free electrons that do not recombine for nanoseconds [9].

Although the fractions of electrons ejected into immediate and solvent-separated contact pairs or as free solvated electrons are visually distinct in Figs. 1b and 2, a model is required to quantitatively extract these fractions from the data. In a previous work, we found that a relatively simple kinetic scheme, which we referred to as the 'delayed ejection' (DE) model, could be used to describe the first ~10 ps of all the pump–probe data for the Na^-/THF system, including scans at probe wavelengths where (unlike the data in Fig. 2) reactive intermediates strongly absorb [8,10]. More recently, we modified the DE model to include the effects of dynamic solvation on the spectroscopy of the reactive intermediates in the Na^- CTTS reaction, which we referred to as the 'delayed ejection plus solvation' (DE + S) model [14]. Although the DE + S model contains more adjustable parameters than the DE model, we found that the DE + S model was able to capture subtleties in the data that were missed by the DE model, and that the DE + S model provided a means to explain some of the early-time dynamics uncovered in the higher-time resolution experiments on Na^-/THF by Ruhman and co-workers [13].

The solid lines passing through the data points in the transient absorption spectra shown in Fig. 2 are fits of the data to the DE + S model. [2] One of the key parameters that can be extracted from the model is p, the fraction of detached electrons that localize in immediate contact pairs. However, for the fraction of electrons that do not recombine in the first few ps, the model does not distinguish between solvent-separated contact pairs and free electrons. We expect that the ~200-ps recombination of the electrons in solvent-separated pairs would be best described as diffusion on a potential of mean force, similar to the analysis performed by Bradforth and co-workers [18] for the recombination of electrons photodetached from aqueous iodide. Until mixed quantum/classical MD simulations presently underway in our group provide the potential of mean force for the Na^-/THF system [19], we can take a much simpler definition of the fraction of electrons that localize into solvent-separated contact pairs based on the separation of time scales evident in Figs. 1b and 2. Since the recombination of solvent-separated pairs ap-

[2] The fit to the 780-nm pump/1500-nm probe data does not reproduce the fast rise, which is due to an instrument-limited sodide p-to-p excited-state absorption at this wavelength, described in detail in [14], that is not taken into account by the model. The data in Fig. 2 can be fit equally well with either the DE or DE + S models, although the DE model results in values for the fraction of immediate contact pairs, p, at wavelengths blue of ~500 nm that are 10–15% higher than the corresponding values from the DE + S model.

Table 1
Fraction of immediate contact pair electrons, solvent-separated pair electrons, and free electrons as a function of excitation wavelength from fits to the data in Fig. 2. The uncertainties are two standard deviations.

Pump λ (nm)	p (immediate)	q (solvent-separated)	r (free)
910	0.986 ± 0.022	0.014 ± 0.031	0.000 ± 0.022
780	0.918 ± 0.010	0.033 ± 0.014	0.049 ± 0.010
641	0.909 ± 0.014	0.036 ± 0.019	0.055 ± 0.013
615	0.684 ± 0.010	0.109 ± 0.018	0.207 ± 0.015
573	0.808 ± 0.016	0.063 ± 0.020	0.129 ± 0.012
555	0.695 ± 0.006	0.099 ± 0.019	0.206 ± 0.018
500	0.566 ± 0.014	0.139 ± 0.017	0.295 ± 0.010
480	0.661 ± 0.026	0.095 ± 0.032	0.244 ± 0.018
460	0.394 ± 0.004	0.197 ± 0.010	0.409 ± 0.009
400	0.334 ± 0.014	0.109 ± 0.024	0.557 ± 0.019

pears complete by 300 ps, we define the fraction of free solvated electrons r as the average of the (properly scaled) pump–probe signals at times longer than 300 ps. The fraction of electrons localized in solvent-separated pairs, q, is then given simply by [3]: $q = 1 - p - r$.

With these definitions in hand, it is straightforward to extract the relative fractions of immediate, solvent-separated and free electrons from the data in Fig. 2; the values of p, q and r for each of the 10 excitation wavelengths are presented in Table 1 and summarized in Fig. 3 (symbols). In particular, the squares in Fig. 3a show the fraction r of free electrons produced via CTTS photodetachment of Na^- as a function of excitation wavelength. The solid curve in Fig. 3a shows a second data set based upon the photodetachment cross-section of Rb^- in THF measured by Levanon and co-workers [7]. To generate this solid curve, an offset of 0.025 was subtracted from the photodetachment cross-section data from [7], and the result was then scaled by a factor of 10. In addition, we have shifted the abscissa of the data from [7] by 0.354 eV, the difference in energy between the absorption maxima for the CTTS bands of Na^- and Rb^- in THF [20]. With this treatment,

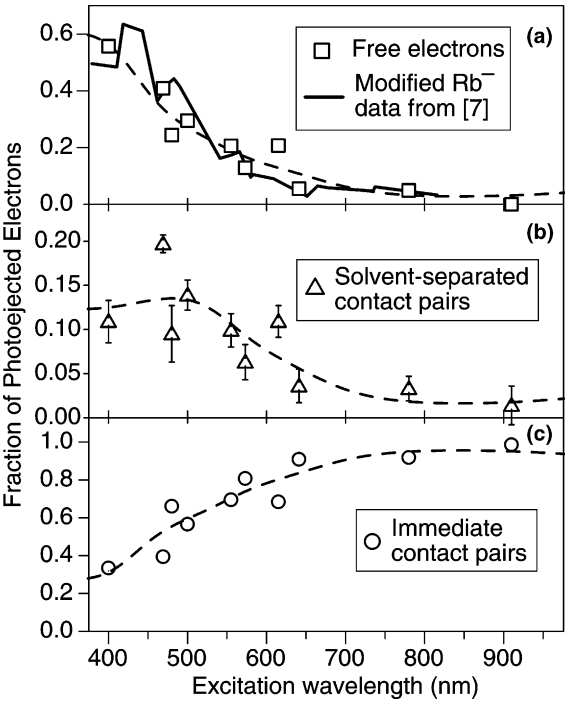

Fig. 3. Photoejection quantum yields as a function of excitation wavelength for different types of electrons following excitation into the CTTS band of Na^- in THF: free electrons (panel (a), squares); electrons in solvent-separated contact pairs (panel (b), triangles); electrons in immediate contact pairs (panel (c), circles). The error bars in panel (b) represent two standard deviations; the corresponding error bars in panels (a) and (c) are smaller than the data symbols. The dashed curves in each panel are fits of the Gaussian sub-bands that constitute the Na^- CTTS absorption spectrum (cf. Fig. 1a) to the data (symbols) using Eqs. (1) and (2). The solid curve in (a) shows data from [7] for the quantum yield of photodetached electrons from the Rb^-/THF CTTS reaction; the data from [7] have been shifted in energy, scaled, and offset; see text for details.

[3] This analysis assumes that upon excitation, electrons are partitioned into one of the three distinct species and do not interconvert. The experimental data do not allow us to determine whether or not interconversion occurs, but the large separation of recombination time scales strongly suggests distinct identities for each of the three species following photoejection.

the offset and scaled Rb^- photodetachment quantum yield values as a function of excitation energy match, within the signal to noise, the fraction of free electrons produced via CTTS of Na^-.

Although it makes sense that the photodetachment cross-sections of Rb^- should be related to the number of free electrons produced by CTTS excitation of Na^-, why do the photodetachment cross-sections need to be modified to compare to the pump–probe data? We believe that the non-zero offset in the photodetachment cross-section observed by Levanon and co-workers at low excitation energies is likely the result of field-induced ionization of the CTTS-excited Rb^-: the 1700 V/cm bias in Levanon and co-workers [7] experiment should be more than adequate to separate some of the electrons localized in immediate or solvent-separated contact pairs that otherwise would have recombined. The scaling factor of 10 needed to make the detachment cross-section of Rb^- match the free electron yield of Na^- likely stems from the limited time resolution of the photoconductivity measurements used to measure the detachment cross-sections [7]: it makes sense that ~90% of the free electrons can undergo diffusive recombination during the ~20-ns instrument response of Levanon and co-workers' photoconductivity apparatus [9]. Although these ideas are somewhat speculative, Fig. 3a strongly suggests that the functional form of the rubidide photodetachment data is related in a simple linear fashion to the fraction of free electrons produced via CTTS excitation of sodide.

The fact that only a simple energy shift of Levanon and co-workers' photodetachment data can bring the two data sets into agreement is also significant. The required shift is exactly equal to the separation of the absorption maxima of Rb^- and Na^-, implying that the electronic structure of the excited CTTS states are similar for both these alkali anions and that only the ground state energy is significantly different between them. This is reasonable in light of recent theoretical work investigating the nature of CTTS excited states of aqueous iodide: the CTTS excited states were found to be stabilized entirely by the polarization of the surrounding solvent molecules [21,22]. We expect that this reasoning can be extended to alkalide/THF CTTS systems, so that the solvent-supported p-like CTTS excited states are largely independent of the identity of the alkali metal atom core; the s-like ground states show a relative shift in energy due to differences in the electron affinities of the different alkalis and to solvatochromic effects.

The estimated photodetachment fractions summarized in Table 1 and Fig. 3 also allow us to investigate the relationship between the three sub-bands we had used to describe the polarization dependence of the bleach recovery of the Na^- CTTS band (Fig. 1a) [14] and the different detachment channels that produce immediate, solvent-separated or free electrons. We start with the assumption that excitation of each sub-band produces a specific quantum yield $\phi_{i,j}$ of each type of electron, where i denotes the Gaussian band that is excited (and takes on values 1–4, with 1 as the lowest-energy sub-band), and j denotes the type of electron produced (taking on values of p, q, or r, for immediate pairs, solvent-separated pairs, or free electrons, respectively). We can then write the fraction of electrons that localize in immediate contact pairs as a function of excitation energy, $p(\varepsilon)$, as:

$$p(\varepsilon) = \frac{\sum_{i=1}^{4} g_i(\varepsilon)\phi_{i,p}}{\sum_{i=1}^{4} g_i(\varepsilon)}, \tag{1}$$

where $g_i(\varepsilon)$ is the amplitude the ith Gaussian band contributing to the total Na^- spectrum at energy ε, and the fractions $q(\varepsilon)$ and $r(\varepsilon)$ for solvent-separated and free electrons are defined analogously. The 12 quantum yields $\phi_{i,j}$ are varied to obtain the best least-squares fit to the data in Table 1, subject to the constraint that for each sub-band i,

$$\sum_{j=p,q,r} \phi_{i,j} = 1. \tag{2}$$

These fits are shown as the dashed curves in Fig. 3, and the corresponding quantum yields of immediate, solvent-separated and free electrons produced by excitation into each of the Gaussian sub-bands are summarized in Table 2. Using this scheme, we also can define the action spectrum for producing each type of detached electron as:

$$F_j(\varepsilon) = \sum_{i=1}^{4} g_i(\varepsilon)\phi_{i,j}. \tag{3}$$

Table 2
Quantum yields of immediate contact pairs (p), solvent-separated contact pairs (q), and free electrons (r) produced upon excitation of each of the four Gaussian sub-bands under the CTTS absorption of sodide in THF; see text for details.

Quantum yield	Gaussian sub-band			
	g_1	g_2	g_3	g_4
ϕ_p	1.00 ± 0.15	0.86 ± 0.14	0.65 ± 0.11	0.27 ± 0.15
ϕ_q	0.00 ± 0.15	0.04 ± 0.14	0.14 ± 0.11	0.12 ± 0.15
ϕ_r	0.00 ± 0.15	0.10 ± 0.14	0.21 ± 0.11	0.61 ± 0.15

Uncertainties are two standard deviations.

Fig. 4 shows the action spectra from Eq. (3) for the production of immediate ($F_p(\varepsilon)$, dashed curve), solvent-separated ($F_q(\varepsilon)$, dot-dashed curves) and free electrons ($F_r(\varepsilon)$, dotted curves). Fig. 4a also shows the experimental Na^- CTTS band (solid curve); from Eqs. (2) and (3), it is clear that the sum of the three action spectra ($\sum_j F_j(\varepsilon)$) is equivalent to the sum of the four Gaussian component sub-bands, which in turn is equal to the total Na^- absorption spectrum.

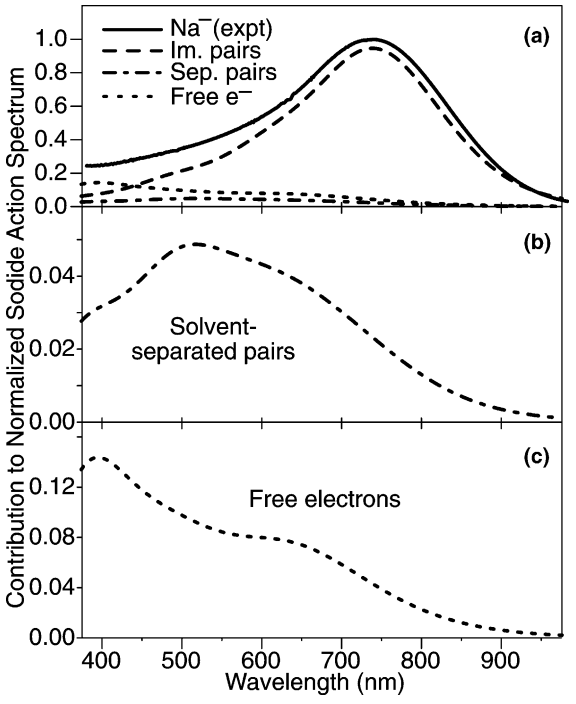

Fig. 4. Normalized action spectra for the production of different types of electrons following excitation of the CTTS band of Na^- in THF: immediate contact pairs (dashed curve); solvent-separated contact pairs (dot–dashed curve); and free electrons (dotted curve). The sum of the three action spectra matches the sum of the four Gaussian bands that describe the experimental absorption spectrum of Na^-, which is shown as the solid curve in panel (a). Panels (b) and (c), respectively, show the same action spectra for solvent-separated contact pairs and free electrons as in panel a, but on a magnified scale.

The fits in Table 2 and Figs. 3 and 4 indicate that there is nearly a one-to-one correspondence between the Gaussian bands used to explain the polarized bleach recovery of the CTTS band [13,14] and the detachment yields for the different types of electrons. Figs. 3c and 4a show that the two lowest-energy sub-bands produce almost exclusively immediate contact pairs, consistent with the idea proposed by Levanon and co-workers [7] that excitation into the low-energy side of the band leads to CTTS rather than direct electron detachment. This emphasizes the contrast between CTTS (localized ejection) and direct photodetachment, in which the electron can localize far from its parent [9].

Figs. 3b and 4b show that the fraction of solvent-separated contact pairs produced at any excitation wavelength is fairly small, reaching only $\sim$10% even for excitation into the highest-energy sub-band. This indicates that the formation of solvent-separated pairs via CTTS detachment is a relatively rare event. The fact that the solvent-separated contact pair formation turns on at about the same energy as production for free electrons suggests that separated pairs form only when there is both enough energy to completely detach the electron and there is a pre-existing trap one solvent shell away from the initially excited sodide anion. [4]

[4] Alternatively, some of the free electrons that we observe at low excitation energies might have formed from the dissociation of solvent-separated pairs; see footnote #3.

At higher excitation energies, the relative yield of free electrons outstrips that of solvent-separated electrons because the increased excitation energy is more than enough to overcome localization into nearby solvent-separated traps. This idea will be tested in upcoming quantum simulations of the Na^- CTTS detachment process [19]. Thus, production of solvent-separated pairs appears to be a relatively rare event for excitations that would otherwise produce free electrons.

Figs. 3 and 4 and Table 2 also show that the fourth (highest-energy) sub-band, which we had crudely assigned previously as absorption into the continuum [14], is primarily responsible for the production of free electrons, although appreciable numbers of immediate contact pair electrons are also produced. In contrast, excitation into the third sub-band appears to produce a mixture of immediate contact pairs and free electrons (as well as a few solvent-separated pairs). Fig. 4 suggests that a one-to-one correspondence between the detachment and polarization sub-bands could be attained by choosing a different functional form for the shapes of the third and fourth bands instead of assuming homogeneously broadened Gaussians [14]. Taken together, the fractions of free electrons, solvent-separated pairs, and immediate contact pairs as a function of excitation wavelength suggest that for the Na^-/THF CTTS system, electrons are detached into different solvent environments depending largely upon the excitation energy and the relative populations of the sub-bands that are initially populated upon excitation.

This idea of distinct sub-bands leading to distinct detachment channels is also consistent with recent work by Bradforth and co-workers [18] on the analogous I^-/water CTTS system. Using both quantum chemical calculations [22] and the experimental observation that the detachment yield for free electrons is independent of excitation wavelength [18], Bradforth and co-workers have argued that the CTTS manifold of I^- consists of absorption to a single excited state. Since the symmetry of I^- is reversed from that of Na^- (I^- has a p-like ground state manifold with a presumably s-like CTTS excited state) it makes sense that electrons detached from I^- via CTTS do so from a single sub-band, resulting in the same quantum yield for all wavelengths.

In summary, the data presented here, combined with the fit of the sodide ground state absorption spectrum to Gaussian sub-bands corresponding to three p-like states plus the continuum [14], allow us to speculate on how the selective excitation of each sub-band determines the fate of the CTTS detached electrons. The quantum yield for production of free solvated electrons from Na^- matches well with the Rb^- photodetachment work by Levanon and co-workers [7], suggesting a similar origin for the onset of the conduction band for the alkali metal anions in THF. The energy shift and scaling we needed to compare the two data sets make sense based on the difference in the absorption maxima of Na^- and Rb^- as well as the differences in time resolution between our two experiments. Although we could not be definite, the evidence suggests that the low fraction of solvent-separated contact pairs upon excitation into the conduction band results from the low probability that an appropriate trap for the solvent-separated electron exists at the time of excitation. Electrons in immediate contact pairs are the primary product of excitation into the middle and lowest-energy p-like excited states, and are likely the major product of excitation into the highest-energy p-like state. Thus, we have a strong indication that the three bands necessary to understand the polarization anisotropy of the Na^- CTTS state are also what determine the fate of the electrons produced by photodetachment.

Acknowledgements

We thank Ignacio B. Martini and Molly C. Cavanagh for assistance in collecting the 910-nm excitation/490-nm probe data shown in Fig. 2a, and Ignacio B. Martini, Ernő Keszei, and Peter Nishimura for critical comments on the manuscript. This work was supported by the National Science Foundation under Grant CHE-0240776. B.J.S. is a Cottrell Scholar of Research Corporation and a Camille Dreyfus Teacher-Scholar. We thank the referee for making us aware of [15].

References

[1] See, e.g., H. Massey, Negative Ions, Cambridge University Press, Cambridge, 1976.
[2] See, e.g., D.M. Neumark, Phys. Chem. Commun. 5 (2002) 76.
[3] See, e.g., A. Sanov, W.C. Lineberger, Phys. Chem. Commun. 5 (2002) 165.
[4] See, e.g., V.H. Vilchiz, J.A. Kloepfer, A.C. Germaine, V.A. Lenchenkov, S.E. Bradforth, J. Phys. Chem. A 105 (2001) 1711.
[5] M.U. Sander, K. Luther, J. Troe, Ber. Bunsenges. Phys. Chem. 97 (1993) 953.
[6] M.J. Blandamer, M.A. Fox, Chem. Rev. 70 (1970) 59.
[7] V. Rozenshtein, Y. Heimlich, H. Levanon, J. Phys. Chem. A 105 (2001) 3701.
[8] E.R. Barthel, I.B. Martini, B.J. Schwartz, J. Chem. Phys. 112 (2000) 9433.
[9] I.B. Martini, E.R. Barthel, B.J. Schwartz, J. Chem. Phys. 113 (2000) 11245.
[10] E.R. Barthel, I.B. Martini, B.J. Schwartz, J. Phys. Chem. B 105 (2001) 12330.
[11] I.B. Martini, E.R. Barthel, B.J. Schwartz, Science 293 (2001) 462.
[12] I.B. Martini, E.R. Barthel, B.J. Schwartz, J. Am. Chem. Soc. 124 (2002) 7622.
[13] Z. Wang, O. Shoshana, B. Hou, S. Ruhman, J. Phys. Chem. A 107 (2003) 3009.
[14] E.R. Barthel, I.B. Martini, E. Keszei, B.J. Schwartz, J. Chem. Phys. 118 (2003) 5916.
[15] J.E. Hendrikson, W.P. Pratt Jr., C.-T. Kuo, Q. Xie, J.L. Dye, J. Phys. Chem. 100 (1996) 3395.
[16] J.L. Dye, J. Phys. Chem. 84 (1980) 1084.
[17] T.-Q. Nguyen, I.B. Martini, J. Liu, B.J. Schwartz, J. Phys. Chem. B 104 (2000) 237.
[18] J.A. Kloepfer, V.H. Vilchiz, V.A. Lenchenkov, X. Chen, S.E. Bradforth, J. Chem. Phys. 117 (2002) 766.
[19] C.J. Smallwood, R.E. Larsen, W.J. Bosma, B.J. Schwartz, submitted for publication.
[20] W.A. Seddon, J.W. Fletcher, F.C. Sopchyshyn, E.B. Selkirk, Can. J. Chem. 57 (1979) 1792.
[21] H.Y. Chen, W.-S. Sheu, Chem. Phys. Lett. 353 (2002) 459.
[22] S.E. Bradforth, P. Jungwirth, J. Phys. Chem. A 106 (2002) 1286.